A&A 473, L37–L40 (2007)
DOI: 10.1051/0004-6361:20078342

Astronomy & Astrophysics

Letter to the Editor

Line shift, line asymmetry, and the ^{6}Li/^{7}Li isotopic ratio determination⋆,⋆⋆

R. Cayrel[1], M. Steffen[2], H. Chand[3], P. Bonifacio[4,5,6], M. Spite[4], F. Spite[4], P. Petitjean[3], H.-G. Ludwig[4,5], and E. Caffau[4]

[1] GEPI, Observatoire de Paris, CNRS, Université Paris Diderot, 61 Av. de l'Observatoire, 75014 Paris, France
[2] Astrophysikalisches Institut Potsdam, An der Sternwarte 16, 14482 Potsdam, Germany
[3] Institut d'Astrophysique de Paris, 98bis bd Arago, 75014 Paris, France
[4] GEPI, Observatoire de Paris, CNRS, Université Paris Diderot, Place Jules Janssen, 92190 Meudon, France
e-mail: Piercarlo.Bonifacio@obspm.fr
[5] CIFIST, Marie Curie Excellence Team
[6] Istituto Nazionale di Astrofisica, Osservatorio Astronomico di Trieste, via Tiepolo 11, 34143 Trieste, Italy

Received 24 July 2007 / Accepted 27 August 2007

ABSTRACT

Context. Line asymmetries are generated by convective Doppler shifts in stellar atmospheres, especially in metal-poor stars, where convective motions penetrate to higher atmospheric levels. Such asymmetries are usually neglected in abundance analyses. The determination of the ^{6}Li/^{7}Li isotopic ratio is prone to suffering from such asymmetries, as the contribution of ^{6}Li is a slight blending reinforcement of the red wing of each component of the corresponding ^{7}Li line, with respect to its blue wing.
Aims. The present paper studies the halo star HD 74000 and estimates the impact of convection-related asymmetries on the Li isotopic ratio determination.
Methods. Two methods are used to meet this aim. The first, which is purely empirical, consists in deriving a template profile from another element that can be assumed to originate in the same stellar atmospheric layers as Li I, producing absorption lines of approximately the same equivalent width as individual components of the ^{7}Li I resonance line. The second method consists in conducting the abundance analysis based on NLTE line formation in a 3D hydrodynamical model atmosphere, taking into account the effects of photospheric convection.
Results. The results of the first method show that the convective asymmetry generates an excess absorption in the red wing of the ^{7}Li absorption feature that mimics the presence of ^{6}Li at a level comparable to the hitherto published values. This opens the possibility that only an upper limit on ^{6}Li/^{7}Li has thus far been derived. The second method confirms these findings.
Conclusions. From this work, it appears that a systematic reappraisal of former determinations of ^{6}Li abundances in halo stars is warranted.

Key words. hydrodynamics – line: profiles – stars: abundances – stars: population II – stars: individual: HD 74000

1. Introduction

Hydrodynamical simulations of stellar atmospheres, including an ab initio treatment of convection, have reached a stage where line profiles are accurately predicted from the Doppler shifts induced by convective motions (Stein & Nordlund 1998; Asplund et al. 2000). The present state of the art is described in the third edition of the book "The Observation and Analysis of Stellar Photospheres" (Chap. 17) by David Gray (2005). The effect of convection, through Doppler shift, on the shape of the atmospheric absorption lines, is to create asymmetric profiles. This has no consequence on abundance determination from isolated lines since a numerical integration over the profile gives the correct equivalent width. Problems arise when one is interested in an unresolved blend. This is the case for the measurement of ^{6}Li/^{7}Li isotopic ratios, which makes use of the ^{6}Li + ^{7}Li blend, where both the presence of ^{6}Li and the line asymmetry caused by convection result in the reinforcement of the red wing of the ^{7}Li feature. Curiously, the consequences of the line asymmetry induced in turn-off (TO) metal-poor halo stars, in which most detections of ^{6}Li have been made, have not been studied in detail. Since ^{6}Li, unlike ^{7}Li, is not (or barely) formed in the standard big bang nucleosynthesis, its presence in metal-poor stars requires a suitable production channel. From a different perspective, the presence of ^{6}Li in metal-poor stars poses strong constraints on any theory of Li depletion in such stars, since ^{6}Li is destroyed by nuclear reactions at lower temperatures than ^{7}Li. Proposals of ^{6}Li production mechanisms to explain the observations in Pop II stars include: decaying massive particles at the time of nucleosynthesis, variations of the fundamental physical constants, structure formation shocks and solar-like flares. The implications of some of these are far reaching and it is therefore of great importance to make the measurements as robust as possible. The study of the impact of line asymmetries on measured Li isotopic ratios is here performed, first observationally, from an empirical point of view, and second, theoretically, by computing the ^{6}Li/^{7}Li blend from a 3D hydrodynamical model atmosphere in order to corroborate the empirical result. We have chosen to perform our observational investigation on the TO metal-poor star HD 74000 because only two upper limits to its ^{6}Li/^{7}Li ratio

⋆ Based on observations carried out at the European Southern Observatory (ESO), under prog. ID 75.D-0600.
⋆⋆ Tables 1–3, and additional references are only available in electronic form at http://www.aanda.org

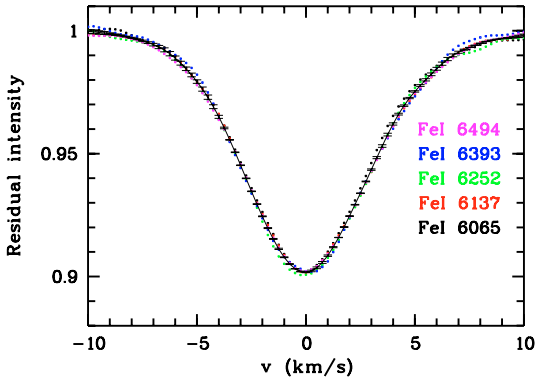

Fig. 1. The profiles of the five selected iron lines after rescaling. Their mean (solid line) and the median profiles are practically identical.

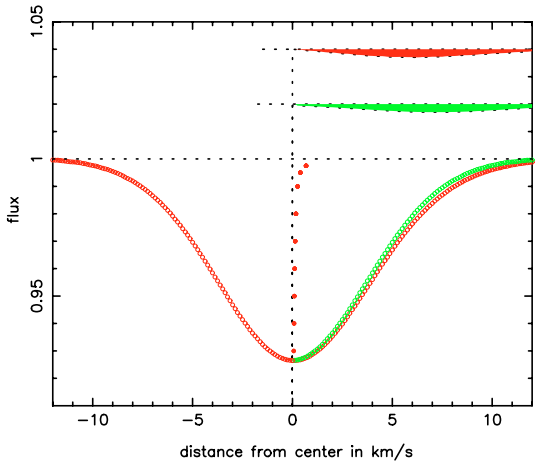

Fig. 2. Asymmetry expected on the main component of the ^{7}Li doublet from the mean profile of the 5 iron lines of Fig. 1. The asymmetric profile is represented by red circles. The symmetric profile of the blue wing is represented by green circles. The excess absorption in the true profile compared to the symmetric red wing is shown with the continuum shifted to 1.04 for clarity. The effect of a ^{6}Li blend corresponding to a ^{6}Li/^{7}Li of 4% is also shown, with the continuum at 1.02, as reference. The two features are strikingly similar, both in size and position. The full red dots mark the line bisector.

exist (Hobbs & Thorburn 1997; Smith et al. 1998) and because this star lies extremely close, in the HR-diagram, to HD 84937, the archetype of a star with measurable ^{6}Li. Twenty one-hour exposures of HD 74000 were obtained with HARPS (Mayor et al. 2003) in service mode at ESO La Silla (Chile). We combined individual exposures into a single spectrum after realignment in wavelength compensating for the Earth's motion. The resulting spectrum has a S/N ratio of 600 per pixel and a spectral resolution of 120 000. Section 2 deals with the observational study, whereas Sect. 3 is a 3D-NLTE study of the formation of the 6708 Å ^{6}Li+^{7}Li blend, essentially to investigate the asymmetry in the line profile induced by the hydrodynamic motions. This aids in understanding the empirical results. Section 4 gives the conclusions of the work.

2. Line asymmetry derived from observation

The goal is to derive a template profile from single component absorption lines that are assumed to arise in the same atmospheric layers as the Li I lines and have similar characteristics. In particular, the lower level of the transition should be at about 5.392 eV from the ionisation level. Several Fe I lines satisfy this constraint and have, in addition, similar line equivalent widths as the main ^{7}Li component of the blend, i.e. about 16 mÅ accounting for 2/3 of the total equivalent width of the Li feature, measured to be 26 mÅ in HD 74000. We have added a third constraint on the wavelength; it should not be too far from that of the Li blend so as to have a similar continuous opacity. Wavelengths shorter than 6700 Å were favoured since the fringing is increasing towards the red. Table 1 lists the five chosen transitions, their wavelength, excitation energy, observed full width half-maximum ($FWHM$) and equivalent width.

We started by convolving the five individual profiles by a Gaussian profile with $FWHM = 1$ km s^{-1} (or about 22 mÅ) slightly larger than the pixel size (17 mÅ). This reduces the photon noise without significant loss of resolution (the isotopic separation of ^{6}Li and ^{7}Li is 0.16 Å or 7.15 km s^{-1}). The absorption lines are then rebinned on a velocity scale with zero velocity fixed at the place of maximum line depth and a step of 0.25 km s^{-1}. The line centre is obtained by a Gaussian fit to the line core. The depressions are finally scaled linearly to the same central value. Figure 1 gives the result of the scaling for the five selected iron lines. The variation of the continuous opacity of H$^-$ between 6000 Å and 6700 Å is very small (about 1%) and does not significantly affect the Fe I and Li I absorptions. To combine the profiles, we allow for variations in central wavelengths and line depths. The final template profile was determined by a simultaneous least square fit of the scaling and shifts of the five lines.

Before discussing more specifically the ^{6}Li/^{7}Li ratio, we have to adapt the profile derived from Fe I to Li I. Indeed, due to different atomic weights, the Li I lines are broader. For a temperature of 5500 K, the line-of-sight thermal broadening $\sqrt{(kT/m)}$ is 0.9 km s^{-1} for ^{56}Fe, 2.55 km s^{-1} for ^{7}Li, and 2.76 km s^{-1} for ^{6}Li. The profile derived from Fe I lines must be convolved with a Gaussian profile of width 2.39 (resp. 2.61) km s^{-1} (5.6, resp. 6.1 km s^{-1} $FWHM$) to be adapted to the ^{7}Li (resp. ^{6}Li) components of the Li blend. Figure 2 shows this convolved profile (red circles).

The asymmetry of the mean profile is usually described by the so-called bisector, which is the locus of the mid-points of horizontal line segments joining the two points of the profile at equal residual intensity, on the blue and red wings. For a symmetric line, the bisector is a straight vertical line.

In Fig. 2 we illustrate the asymmetry of our derived mean profile by plotting the mirror image of the left wing with respect to the vertical line at the centre. It is apparent that an excess absorption exists in the red wing. The difference between the red wing and the mirror of the blue wing is shown with the continuum shifted to 1.04. For comparison, we show the depression of a line representing 4% of the main line equivalent width, with the continuum shifted to 1.02 (see figure). The quasi-degeneracy between these two signals is the central problem we address in this paper. If one ignores the asymmetry in the modelling of the absorption feature (which is the case in all 1D-LTE analyses), one will overestimate the strength of the component blended in the red wing, and hence derive a spurious ^{6}Li abundance.

To compute an empirical profile of the Li I resonance doublet we assumed that the individual line components (doublet, isotopic, hyperfine) have the same shape as the observed mean iron profile. We further assumed that they are located at the same wavelengths and have the same gf-values as used by Asplund et al. (2006). Each component was weighted by its gf-value and the abundance of ^{6}Li or ^{7}Li. Our fitting parameters were

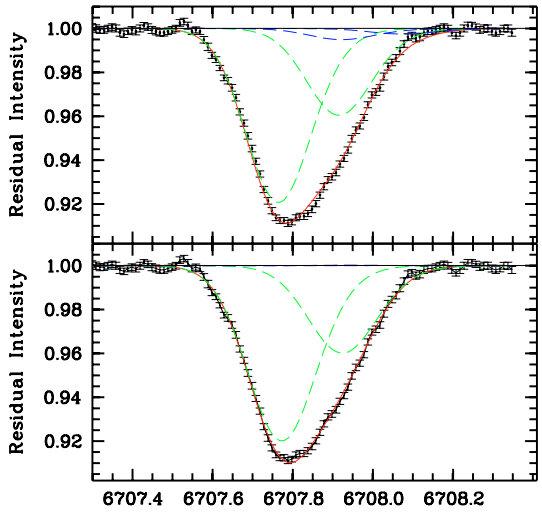

Fig. 3. *Upper panel*: the observed Li doublet (black dots with error bars), together with the best fitting synthetic profile (red solid line) computed using the empirical profile derived from the Fe I lines. The green dashed lines show the ^{7}Li components and the blue dashed lines the ^{6}Li components. Fitting parameters are the contributions of ^{7}Li and ^{6}Li and thermal broadening, but no global wavelength shift was allowed. See text for details. *Lower panel*: like upper panel, but also allowing for a global wavelength shift, the best fit corresponds to a shift of 372 m s^{-1}.

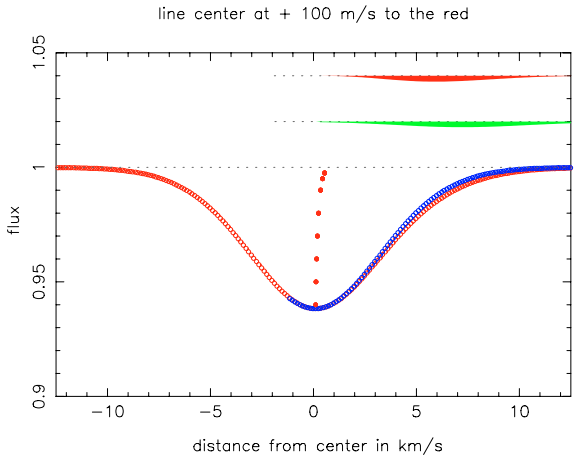

Fig. 4. Profile of a single component of ^{7}Li computed with Linfor3D in LTE. It is based on the average over 11 snapshots from a CO^{5}BOLD model atmosphere run with $T_{\rm eff}$ = 6375 K, log (g) = 4.0, [Fe/H] = −2.0. The asymmetry is characterised by the difference between the red wing (circles) and the mirror image of the blue wing (blue circles) The area between both is shown in red at the top, as in Fig. 2. The asymmetry is 3% in area, and the convective line shift is 100 m/s to the red.

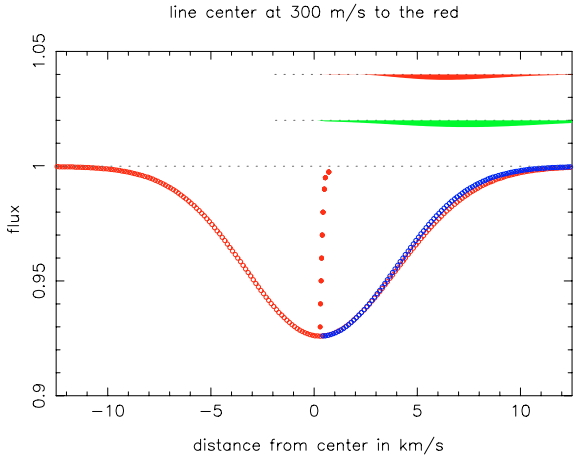

Fig. 5. Like Fig. 4 but for the case of 3D-NLTE. The convective shift is 3 times larger and the area asymmetry slightly less.

therefore the two abundances, an additional thermal broadening and a global velocity shift of the whole absorption profile to allow for uncertainties in the wavelength calibration.

Figure 3 displays the results of our fits to the observed resonance Li I doublet in HD 74000 (see also Table 2). We note that scanning of the χ^2 in parameter space, as well as Monte Carlo simulations, show that isotopic ratio, velocity shift and thermal broadening are correlated parameters. The fit in which all the parameters are left free requires an emission of the ^{6}Li component. This is, of course, unphysical and must be interpreted as evidence that when the empirical asymmetric profile is used there is no need for a contribution by ^{6}Li. In the upper panel, the velocity shift is fixed to zero, the low goodness of fit in this case makes the fit, at most, marginally acceptable. On the other hand, it can be seen from Table 2 that a fit with ^{6}Li fixed to zero is good, confirming that the assumption of the absence of ^{6}Li allows an acceptable fit. To assess the impact of the line asymmetry on the derived ^{6}Li/^{7}Li ratio, we constructed a symmetric profile by mirroring the blue wing of our empirical profile, which matches the unblended part of the ^{7}Li component. This results in a good fit (not displayed here), but requires an isotopic ratio of 2.3%.

Our conclusion, based on the use of the asymmetric empirical profile, is that there is no positive detection of ^{6}Li in HD 74000.

3. Effects of line asymmetries from theoretical 3D-NLTE simulations

To corroborate our empirical findings, we performed a theoretical investigation of the line formation process based on a 3D hydrodynamical model atmosphere. Spectrum synthesis calculations of the Li feature were first performed assuming LTE, and subsequently by applying a 3D-NLTE code to study the impact of departures from LTE on the resulting line profile.

A synthetic spectrum was calculated with the code Linfor3D developed in Potsdam and Meudon[1]. The spectrum is based on an average over 11 independent snapshots (each representing 28 × 28 Mm^2 of the stellar surface with 140 × 140 grid points) generated by the radiation-hydrodynamics code CO^{5}BOLD (Freytag et al. 2002; Wedemeyer et al. 2004). The atmospheric parameters of the model are $T_{\rm eff}$ = 6375, log g = 4.0 and metallicity −2.0, as shown in Table 3, together with a selection of parameters found in the literature The result is shown in Fig. 4. The asymmetry is very similar in shape and size to the one obtained from the empirical observational study.

We have repeated the same computation using the same snapshots, applying this time a 3D-NLTE code newly developed by two of us (Steffen and Cayrel). The code uses an 8 level Li I model atom including 11 transitions and the corresponding radiative processes, electron collisions and the Li+H charge exchange process computed by Barklem et al. (2003). Figure 5 shows the resulting line profile, slightly less asymmetric than the one obtained under the 3D-LTE assumption, but still exhibiting an asymmetry equivalent to a ^{6}Li/^{7}Li ratio blend of 2.7%, comparable to the value derived in our empirical study.

A completely new aspect has been brought to light by the 3D-NLTE study: there is a drastic change of the contribution function to the equivalent width in 3D-NLTE with respect to

[1] http://www.aip.de/~mst/Linfor3D/linfor_3D_manual.pdf

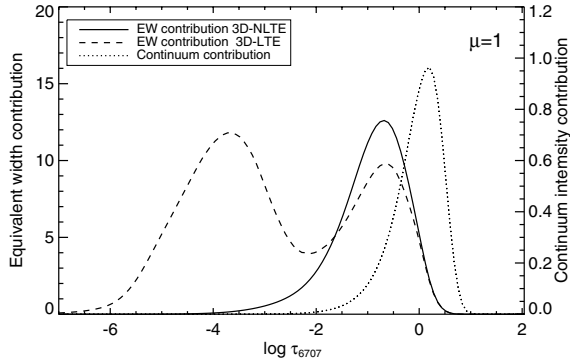

Fig. 6. The contribution functions of the (disk-centre) equivalent width of the Li I 6707.8 Å line (solid lines, left ordinate) and of the (disk-centre) continuum intensity (dotted line, right ordinate) in 3D-LTE and 3D-NLTE. Note the double peak in the equivalent width contribution function in 3D-LTE for the Li line. The peak at the surface is due to an increased LTE population of the levels at the low surface temperatures reached in the 3D model. In 3D-NLTE, the departures from LTE completely annihilate this peak and strengthen the inner peak.

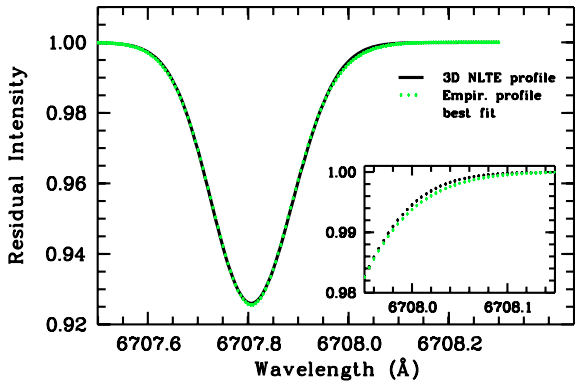

Fig. 7. Comparison between empirical and 3D-NLTE profile.

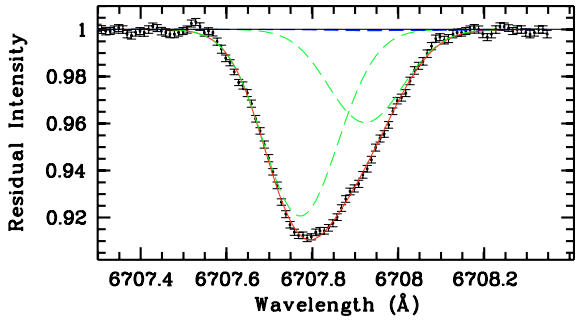

Fig. 8. Fit with 3D-NLTE profile providing ^{6}Li/^{7}Li = 0.6%.

3D-LTE (see Fig. 6). The contribution of the very cool surface layers has been removed by departure coefficients of about 1/100, reducing the equivalent width of the full ^{6}Li+^{7}Li feature from 59 mÅ to 23 mÅ for the standard abundance of ^{7}Li of 2.2 ($\log(nH) = 12$ scale). Linked to this change, the ^{7}Li and ^{6}Li line central wavelengths have been redshifted by 7 mÅ, or about 300 m s^{-1}. This explains why, during a quarter of a century, it has always been necessary to shift the synthetic feature to the red of its rest-wavelength, a shift largely above the uncertainty in wavelength calibrations with high resolution spectrographs.

Figure 7 illustrates the close correspondence between our empirical (iron line based) Li line profile and the synthetic 3D-NLTE profile. In Fig. 8 we show the result of our best fit using the 3D-NLTE profile as a building-block of the Li feature. The theoretical profile has the correct thermal broadening. We have rotationally broadened the theoretical profile by 1 km s^{-1}, as described in Ludwig (2007), to match the projected rotational velocity of the star. Note that the required additional broadening is 2.66 km s^{-1}, which is very close to the nominal resolution of HARPS. We obtain a ^{6}Li/^{7}Li ratio of 0.6% and estimate the error on the Li isotopic ratio to be 2%. A Monte Carlo simulation, taking into account only Poisson noise, provides an error estimate of 1.6%. Our estimated total uncertainty of 2% takes into account the presence of non-Poisson noise (e.g. residual fringing).

We have computed the asymmetry for LTE and NLTE with a gravity $\log(g) = 4.5$ (see Table 3), instead of 4.0, and found very different results, with an asymmetry 3 times smaller, showing that the asymmetry is very gravity dependent. Obviously computations covering a substantial fraction of the parameters, $T_{\rm eff}$, g and metallicity, are needed.

4. Conclusions

We provide evidence for a significant degree of degeneracy between the asymmetry caused by hydrodynamical effects on the Li I resonance line, and the asymmetry caused by the presence of a ^{6}Li blend. From both an observational study of the spectrum of HD 74000, and 3D-LTE and 3D-NLTE line synthesis computations, we conclude that the size and shape of the convection-related asymmetry is equivalent to a contribution of ^{6}Li by a few percent. We find in HD74000, ^{6}Li/^{7}Li = (0 ± 2)%. Moreover, the 3D-NLTE approach allows us to understand the 6 to 10 mÅ shift commonly needed to fit the observed profile with a 1D synthetic profile.

Strictly taken, our results do not imply that previous measurements of the ^{6}Li/^{7}Li isotopic ratio are invalidated since ^{6}Li has not been previously detected in HD 74000. However, we systematically find smaller isotopic ratios when fitting the observed spectrum with asymmetric line profiles rather than symmetric ones. This is what we expect from the influence of the line asymmetry, but opposite to what Asplund et al. (2006) obtain. The reason for this discrepancy is unclear, but we believe that our study features an unprecedented accuracy by treating line asymmetries in a largely model-independent fashion, working with a spectrum of outstanding S/N ratio, spectral resolution and wavelength accuracy, as well as including NLTE effects in the 3D modelling. Therefore, a serious reappraisal of the ^{6}Li abundances derived from earlier works seems warranted.

References

Asplund, M., Nordlund, Å, Trampedach, R., et al. 2000, A&A, 888, 555
Asplund, M., Lambert, D. L., Nissen, P. E., Primas, F., & Smith, V. V. 2006, ApJ, 644, 229
Barklem, P.S., Belyaev, A.K., & Asplund, M. 2003, A&A, 409, L1
Freytag, B., Steffen, M., & Dorch, B. 2002, AN, 323, 213
Gray, D. F. 2005, The Observation and Analysis of Stellar Photospheres, 3rd edition, ed. D. F. Gray (Cambridge, UK: Cambridge University Press)
Hobbs, L. M., & Thorburn, J. A. 1997, ApJ, 491, 772
Ludwig, H.-G. 2007, A&A, 471, 925
Mayor, M., Pepe, F., Queloz, D., et al. 2003, The Messenger, 114, 20
Nave, G., Johansson, S., Learner, R. C. M., Thorne, A. P., & Brault, J. W. 1994, ApJS, 94, 221
Smith, V. V., Lambert, D. L., & Nissen, P. E. 1998, ApJ, 506, 405
Stein, R. F., & Nordlund, Å1998, ApJ, 499, 914
Wedemeyer, S., Freytag, B., Steffen, M., Ludwig, H.-G., & Holweger, H. 2004, A&A, 414, 1121

Online Material

Table 1. List of selected Fe I lines.

Mult.[a]	Wavelength (Å)	χ_{exc} (eV)	$\chi_{ion} - \chi_{exc}$ (eV)	$FWHM$ (km s^{-1})	EW (mÅ)
536	6065.4822	2.608	5.294	0.129	13.1
536	6137.6920	2.588	5.314	0.136	17.5
465	6252.5554	2.404	5.498	0.135	14.7
464	6393.6013	2.433	5,469	0.140	17.0
464	6494.9805	2.404	5.498	0.142	30.4[b]

[a] Nave et al. (1994). [b] Although stronger than the other lines this scales linearly and provides a higher S/N ratio.

Table 2. Results of the fit to the observed Li I doublet of HD 74000.

Type of fit	^{6}Li/^{7}Li[a] %	Shift[b] m s^{-1}	Broadening km s^{-1}	Goodness of fit[c]
Empirical Prof.	–2.8	371	5.81	0.304
Empirical Prof.	6.3	0[d]	5.15	0.002
Empirical Prof.	0[d]	372	5.77	0.316
Symmetr. Prof.	2.3	412	5.92	0.272
1D LTE	2.4	394	5.80	0.233
3D LTE[e]	0.2	290	4.29	0.324
3D NLTE[e]	0.6	82	2.66	0.303

[a] A negative value indicates that the fitted ^{6}Li line is emission. [b] This is the fitted shift necessary to match the observed profile, note that while the empirical and 1D profiles have a zero intrinsic shift the 3D profiles have +100 m s^{-1} and +300 m s^{-1} convective shifts respectively. [c] Defined as the probability of obtaining a χ^2 as high as the one observed. [d] Fixed. [e] Rotationally broadened by 1 km s^{-1}.

Table 3. Atmospheric parameters of HD 74000.

T_{eff}	log g	[Fe/H]	Ref.
6375	4.00	−2.00	CO^{5}BOLD model
6320	4.50	−2.00	CO^{5}BOLD model
6126	4.01	−1.80	Zhang & Zhao (2005)
6040	4.20	−2.17	Arnone et al. (2005)
6392	4.27	−1.96	Melendez & Ramirez (2004)
6109		−1.96	Nordström et al. (2004)
6203	4.03	−2.05	Gehren et al. (2004)
6216	4.09	−1.96	Gratton et al. (2003)
6025	4.10	−2.0	Fulbright (2000)
6040		−2.02	Ryan et al. (1999)
6190	4.13	−2.00	Smith et al. 1998)
6090	4.00	−2.00	Hobbs & Thorburn (1997)
6184	4.13	−1.69	Nissen et al. (1997)
6224	4.50	−2.00	Alonso et al. (1996)
6341	5.19	−1.52	Gratton et al. (1996)
6090	4.15	−2.08	Beveridge & Sneden (1994)
6211	3.92	−1.93	Axer et al. (1994)
6090	4.35	−1.98	Tomkin et al. (1992)
6146	3.90	−2.23	Magain (1989)
6072	4.2	−2.06	Hartmann & Gehren (1988)
6222	4.5	−1.80	Peterson (1978)

References

Alonso, A., Arribas, S., & Martinez-Roger, C. 1996, A&AS, 117, 227
Arnone, E., Ryan, S. G., Argast, D., Norris, J. E., & Beers, T. C. 2005, A&A, 430, 507
Axer, M., Fuhrmann, K., & Gehren, T. 1994, A&A, 291, 895
Beveridge, R. C., & Sneden, C. 1994, AJ, 108, 285
Fulbright, J. P. 2000, AJ, 120, 1841
Gehren, T., Liang, Y. C., Shi, J. R., Zhang, H. W., & Zhao, G. 2004, A&A, 413, 1045
Gratton, R. G., Carretta, E., & Castelli, F. 1996, A&A, 314, 191
Gratton, R. G., Carretta, E., Claudi, R., Lucatello, S., & Barbieri, M. 2003, A&A, 404, 187
Hobbs, L. M., & Thorburn, J. A. 1997, ApJ, 491, 772
Hartmann, K., & Gehren, T. 1988, A&A, 199, 269
Magain, P. 1989, A&A, 209, 211
Meléndez, J., & Ramírez, I. 2004, ApJ, 615, L33
Nissen, P. E., Hoeg, E., & Schuster, W. J. 1997, Hipparcos - Venice '97, 402, 225
Nordström, B., Mayor, M., Anderson, J., et al. 2004, A&A, 418, 989
Peterson, R. 1978, ApJ, 222, 181
Ryan, S. G., Norris, J. E., & Beers, T. C. 1999, ApJ, 523, 654
Smith, V. V., Lambert, D. L., & Nissen, P. E. 1998, ApJ, 506, 405
Tomkin, J., Lemke, M., Lambert, D. L., & Sneden, C. 1992, AJ, 104, 1568
Zhang, H. W., & Zhao, G. 2005, MNRAS, 364, 712